FRONT COVER PHOTO: Parabolic reflector (25-m diameter) of 27-element Very Large Array (VLA) radio telescope. National Radio Astronomy Observatory (NRAO), Socorro, New Mexico.

ACQUISITIONS EDITOR Steven Elliot
MARKETING MANAGER Jay Kirsch
SENIOR PRODUCTION EDITOR Tony VenGraitis
DESIGNER Harry Nolan
MANUFACTURING MANAGER Mark Cirillo
ILLUSTRATION Jamie Perea
PRODUCTION SERVICE Ingrao Associates
COVER PHOTOGRAPH Socorro Mexico, Telegraph Colour Library FPG. ©

This book was set in *Times Roman* by *Ruttle, Shaw & Wetherill,* and printed and bound by *Hamilton Printing.* The cover was printed by *New England Book Components.*

Recognizing the importance of preserving what has been written, it is a policy of John Wiley & Sons, Inc. to have books of enduring value published in the United States printed on acid-free paper, and we exert our best efforts to that end.

Library of Congress Cataloging in Publication Data:
Balanis, Constantine A., 1938–
Antenna theory : analysis and design / Constantine A. Balanis. — 2nd ed.
p. cm.
Includes index.
ISBN 0–471–59268–4 (cloth : alk. paper)
1. Antennas (Electronics) I. Title.
TK7871.6.B353 1997
621.382'4—dc20

96–12134
CIP

Printed in the United States of America

10 9 8 7 6

Using (3-15) or (3-10) with $\mathbf{J} = 0$, the corresponding electric field components can be written as

$$E_r = E_\theta = 0 \tag{5-19a}$$

$$E_\phi = \eta \frac{(ka)^2 I_0 \sin\theta}{4r}\left[1 + \frac{1}{jkr}\right] e^{-jkr} \tag{5-19b}$$

5.2.2 Small Loop and Infinitesimal Magnetic Dipole

A comparison of (5-18a)–(5-19b) with those of the infinitesimal magnetic dipole indicates that they have similar forms. In fact, the electric and magnetic field components of an infinitesimal magnetic dipole of length l and constant "magnetic" current I_m are given by

$$E_r = E_\theta = H_\phi = 0 \tag{5-20a}$$

$$E_\phi = -j\frac{kI_m l \sin\theta}{4\pi r}\left[1 + \frac{1}{jkr}\right] e^{-jkr} \tag{5-20b}$$

$$H_r = \frac{I_m l \cos\theta}{2\pi\eta r^2}\left[1 + \frac{1}{jkr}\right] e^{-jkr} \tag{5-20c}$$

$$H_\theta = j\frac{kI_m l \sin\theta}{4\pi\eta r}\left[1 + \frac{1}{jkr} - \frac{1}{(kr)^2}\right] e^{-jkr} \tag{5-20d}$$

These can be obtained from the fields of an infinitesimal electric dipole, (4-8a)–(4-10c). When (5-20a)–(5-20d) are compared with (5-18a)–(5-19b), they indicate that *a magnetic dipole of magnetic moment $I_m l$ is equivalent to a small electric loop of radius a and constant electric current I_0 provided that*

$$I_m l = jS\omega\mu I_0 \tag{5-21}$$

where $S = \pi a^2$ (area of the loop). Thus, for analysis purposes, the small electric loop can be replaced by a small linear magnetic dipole of constant current. The geometrical equivalence is illustrated in Figure 5.1(a) where the magnetic dipole is directed along the z-axis which is also perpendicular to the plane of the loop.

5.2.3 Power Density and Radiation Resistance

The fields radiated by a small loop, as given by (5-18a)–(5-19b), are valid everywhere except at the origin. As was discussed in Section 4.1 for the infinitesimal dipole, the power in the region very close to the antenna (near-field, $kr \ll 1$) is predominantly reactive and in the far-field ($kr \gg 1$) is predominantly real. To illustrate this for the loop, the complex power density

$$\begin{aligned}\mathbf{W} &= \tfrac{1}{2}(\mathbf{E} \times \mathbf{H}^*) = \tfrac{1}{2}[(\hat{\mathbf{a}}_\phi E_\phi) \times (\hat{\mathbf{a}}_r H^*_r + \hat{\mathbf{a}}_\theta H^*_\theta)] \\ &= \tfrac{1}{2}(-\hat{\mathbf{a}}_r E_\phi H^*_\theta + \hat{\mathbf{a}}_\theta E_\phi H^*_r)\end{aligned} \tag{5-22}$$

is first formed. When (5-22) is integrated over a closed sphere, only its radial component given by

$$W_r = \eta \frac{(ka)^4}{32}|I_0|^2 \frac{\sin^2\theta}{r^2}\left[1 + j\frac{1}{(kr)^3}\right] \tag{5-22a}$$

contributes to the complex power P_r. Thus

$$P_r = \oiint_S \mathbf{W} \cdot d\mathbf{s} = \eta \frac{(ka)^4}{32}|I_0|^2 \int_0^{2\pi}\int_0^{\pi}\left[1 + j\frac{1}{(kr)^3}\right] \sin^3\theta \, d\theta \, d\phi \tag{5-23}$$

which reduces to

$$P_r = \eta\left(\frac{\pi}{12}\right)(ka)^4 |I_0|^2 \left[1 + j\frac{1}{(kr)^3}\right] \tag{5-23a}$$

and whose real part is equal to

$$P_{\text{rad}} = \eta\left(\frac{\pi}{12}\right)(ka)^4 |I_0|^2 \tag{5-23b}$$

For small values of kr ($kr \ll 1$), the second term within the brackets of (5-23a) is dominant which makes the power mainly reactive. In the far-field ($kr \gg 1$), the second term within the brackets diminishes which makes the power real. A comparison between (5-23a) with (4-14) indicates a difference in sign between the terms within the brackets. Whereas for the infinitesimal dipole the radial power density in the near-field is capacitive, for the small loop it is inductive. This indicates that the radial magnetic energy is larger than the electric energy.

The radiation resistance of the loop is found by equating (5-23b) to $|I_0|^2 R_r/2$. Doing this, the radiation resistance can be written as

$$R_r = \eta\left(\frac{\pi}{6}\right)(k^2a^2)^2 = \eta\frac{2\pi}{3}\left(\frac{kS}{\lambda}\right)^2 = 20\pi^2\left(\frac{C}{\lambda}\right)^4 = 31{,}171\left(\frac{S^2}{\lambda^4}\right) \tag{5-24}$$

where $S = \pi a^2$ is the area and $C = 2\pi a$ is the circumference of the loop.

The radiation resistance as given by (5-24) is only for a single-turn loop. If the loop antenna has N turns wound so that the magnetic field passes through all the loops, the radiation resistance is equal to that of single turn multiplied by N^2. That is,

$$R_r = \eta\left(\frac{2\pi}{3}\right)\left(\frac{kS}{\lambda}\right)^2 N^2 = 20\pi^2\left(\frac{C}{\lambda}\right)^4 N^2 = 31{,}171\, N^2\left(\frac{S^2}{\lambda^4}\right) \tag{5-24a}$$

Even though the radiation resistance of a single turn loop may be small, the overall value can be increased by including many turns. This is a very desirable and practical mechanism that is not available for the infinitesimal dipole.

Example 5.1

Find the radiation resistance of a single-turn and an 8-turn small circular loop. The radius of the loop is $\lambda/25$ and the medium is free-space.

SOLUTION

$$S = \pi a^2 = \pi\left(\frac{\lambda}{25}\right)^2 = \frac{\pi\lambda^2}{625}$$

$$R_r \text{ (single turn)} = 120\pi\left(\frac{2\pi}{3}\right)\left(\frac{2\pi^2}{625}\right)^2 = 0.788 \text{ ohms}$$

$$R_r \text{ (8 turns)} = 0.788(8)^2 = 50.43 \text{ ohms}$$

PROXIMITY EFFECT

The radiation and loss resistances of an antenna determine the radiation efficiency, as defined by (2-90). The loss resistance of a single-turn small loop is, in general, much larger than its radiation resistance; thus the corresponding radiation efficiencies are very low and depend on the loss resistance. To increase the radiation efficiency, multiturn loops are often employed. However, because the current distribution in a multiturn loop is quite complex, great confidence has not yet been placed in analytical methods for determining the radiation efficiency. Therefore greater reliance has been placed on experimental procedures. Two experimental techniques that can be used to measure the radiation efficiency of a small multiturn loop are those that are usually referred to as the *Wheeler method* and the *Q method* [1].

Usually it is assumed that the loss resistance of a small loop is the same as that of a straight wire whose length is equal to the circumference of the loop, and it is computed using (2-90b). Although this assumption is adequate for single-turn loops, it is not valid for multiturn loops. In a multiturn loop, the current is not uniformly distributed around the wire but depends on the skin and proximity effects [2]. In fact, for close spacings between turns, the contribution to the loss resistance due to the proximity effect can be larger than that due to the skin effect.

The total ohmic resistance for an N-turn circular loop antenna with loop radius a, wire radius b, and loop separation $2c$, shown in Figure 5.2(a) is given by [3]

$$R_{\text{ohmic}} = \frac{Na}{b}R_s\left(\frac{R_p}{R_0} + 1\right) \tag{5-25}$$

where

$$R_s = \sqrt{\frac{\omega\mu_0}{2\sigma}} = \text{surface impedance of conductor}$$

$$R_p = \text{ohmic resistance per unit length due to proximity effect}$$

$$R_0 = \frac{NR_s}{2\pi b} = \text{ohmic skin effect resistance per unit length (ohms/m)}$$

The ratio of R_p/R_0 has been computed [3] as a function of the spacing c/b for loops with $2 \le N \le 8$ and it is shown plotted in Figure 5.2(b). It is evident that for close spacing the ohmic resistance is twice as large as that in the absence of the proximity effect ($R_p/R_0 = 0$).

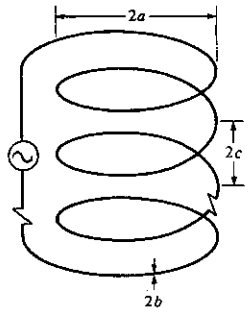

(a) N-turn circular loop

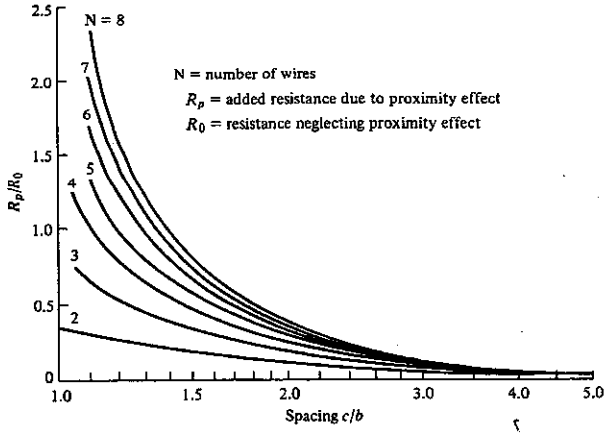

(b) Ohmic resistance due to proximity (after G. N. Smith)

Figure 5.2 N-turn circular loop and ohmic resistance due to proximity effect. (SOURCE: G. S. Smith, "Radiation Efficiency of Electrically Small Multiturn Loop Antennas," *IEEE Trans. Antennas Propagat.*, Vol. AP-20, No. 5, pp. 656-657, Sept. 1972© (1972) IEEE).

Example 5.2

Find the radiation efficiency of a single-turn and an 8-turn small circular loop at $f = 100$ MHz. The radius of the loop is $\lambda/25$, the radius of the wire is $10^{-4}\lambda$, and the turns are spaced $4 \times 10^{-4}\lambda$ apart. Assume the wire is copper with a conductivity of 5.7×10^7 (S/m) and the antenna is radiating into free-space.

SOLUTION

From Example 5.1

$$R_r \text{ (single turn)} = 0.788 \text{ ohms}$$

$$R_r \text{ (8 turns)} = 50.43 \text{ ohms}$$

The loss resistance for a single turn is given, according to (2-90b), by

$$R_L = R_{hf} = \frac{a}{b}\sqrt{\frac{\omega\mu_0}{2\sigma}} = \frac{1}{25(10^{-4})}\sqrt{\frac{\pi(10^8)(4\pi \times 10^{-7})}{5.7 \times 10^7}}$$
$$= 1.053 \text{ ohms}$$

and the radiation efficiency, according to (2-90), by

$$e_{cd} = \frac{0.788}{0.788 + 1.053} = 0.428 = 42.8\%$$

From Figure 5.2(b)

$$\frac{R_g}{R_0} = 0.38$$

and from (5-25)

$$R_L = R_{\text{ohmic}} = \frac{8}{25(10^{-4})}\sqrt{\frac{\pi(10^8)(4\pi \times 10^{-7})}{5.7 \times 10^7}}(1.38) = 11.62$$

Thus

$$e_{cd} = \frac{50.43}{50.43 + 11.62} = 0.813 = 81.3\%$$

5.2.4 Near-Field ($kr \ll 1$) Region

The expressions for the fields, as given by (5-18a)–(5-19b), can be simplified if the observations are made in the near-field ($kr \ll 1$). As for the infinitesimal dipole, the predominant term in each expression for the field in the near-zone region is the last one within the parentheses of (5-18a)–(5-19b). Thus for $kr \ll 1$

$$\left.\begin{aligned} H_r &\simeq \frac{a^2 I_0 e^{-jkr}}{2r^3}\cos\theta && \text{(5-26a)}\\ H_\theta &\simeq \frac{a^2 I_0 e^{-jkr}}{4r^3}\sin\theta && \text{(5-26b)}\\ H_\phi &= E_r = E_\theta = 0 && \text{(5-26c)}\\ E_\phi &\simeq -j\frac{a^2 k I_0 e^{-jkr}}{4r^2}\sin\theta && \text{(5-26d)} \end{aligned}\right\} \quad kr \ll 1$$

The two **H**-field components are in time-phase. However, they are in time quadrature with those of the electric field. This indicates that the average power (real power) is zero, as for the infinitesimal electric dipole. The condition of $kr \ll 1$ can be satisfied at moderate distances away from the antenna provided the frequency of operation is very low. The fields of (5-26a)–(5-26d) are usually referred to as *quasi-stationary*.

5.2.5 Far-Field ($kr \gg 1$) Region

The other space of interest where the fields can be approximated is the far-field ($kr \gg 1$) region. In contrast to the near-field, the dominant term in (5-18a)–(5-19b) for $kr \gg 1$ is the first one within the parentheses. Since for $kr > 1$ the H_r component will be inversely proportional to r^2 whereas H_θ will be inversely proportional to r, for large values of kr ($kr \gg 1$) the H_r component will be small compared to H_θ. Thus it can be assumed that it is approximately equal to zero. Therefore for $kr \gg 1$,

$$\left.\begin{aligned} H_\theta &\simeq -\frac{k^2 a^2 I_0 e^{-jkr}}{4r}\sin\theta = -\frac{\pi S I_0 e^{-jkr}}{\lambda^2 r}\sin\theta && \text{(5-27a)}\\ E_\phi &\simeq \eta\frac{k^2 a^2 I_0 e^{-jkr}}{4r}\sin\theta = \eta\frac{\pi S I_0 e^{-jkr}}{\lambda^2 r}\sin\theta && \text{(5-27b)}\\ H_r &\simeq H_\phi \simeq E_r = E_\theta \simeq 0 && \text{(5-27c)} \end{aligned}\right\} \quad kr \gg 1$$

where $S = \pi a^2$ is the geometrical area of the loop.

Forming the ratio of $-E_\phi/H_\theta$, the wave impedance can be written as

$$Z_w = -\frac{E_\phi}{H_\theta} \simeq \eta \qquad \text{(5-28)}$$

where

Z_w = wave impedance
η = intrinsic impedance

As for the infinitesimal dipole, the **E**- and **H**-field components of the loop in the far-field ($kr \gg 1$) region are perpendicular to each other and transverse to the direction of propagation. They form a *T*ransverse *E*lectro *M*agnetic (TEM) field whose wave impedance is equal to the intrinsic impedance of the medium. Equations (5-27a)–(5-27c) can also be derived using the procedure outlined and relationships developed in Section 3.6. This is left as an exercise to the reader (Prob. 5.5).

5.2.6 Radiation Intensity and Directivity

The real power P_{rad} radiated by the loop was found in Section 5.2.3 and is given by (5-23b). The same expression can be obtained by forming the average power density, using (5-27a)–(5-27c), and integrating it over a closed sphere of radius r. This is left as an exercise to the reader (Prob. 5.4). Associated with the radiated power P_{rad} is an average power density $\mathbf{W}_{\text{av}}$. It has only a radial component W_r which is related to the radiation intensity U by

$$U = r^2 W_r = \frac{\eta}{2}\left(\frac{k^2 a^2}{4}\right)^2 |I_0|^2 \sin^2\theta = \frac{r^2}{2\eta}|E_\phi(r, \theta, \phi)|^2 \qquad \text{(5-29)}$$

and it conforms to (2-12a). The normalized pattern of the loop, as given by (5-29), is identical to that of the infinitesimal dipole shown in Figure 4.2. The maximum value occurs at $\theta = \pi/2$, and it is given by

$$U_{\max} = U|_{\theta=\pi/2} = \frac{\eta}{2}\left(\frac{k^2 a^2}{4}\right)^2 |I_0|^2 \qquad \text{(5-30)}$$

Using (5-30) and (5-23b), the directivity of the loop can be written as

$$D_0 = 4\pi \frac{U_{\max}}{P_{\text{rad}}} = \frac{3}{2} \tag{5-31}$$

and its maximum effective aperture as

$$A_{em} = \left(\frac{\lambda^2}{4\pi}\right) D_0 = \frac{3\lambda^2}{8\pi} \tag{5-32}$$

It is observed that the directivity, and as a result the maximum effective area, of a small loop is the same as that of an infinitesimal electric dipole. This should be expected since their patterns are identical.

The far-field expressions for a small loop, as given by (5-27a)–(5-27c), will be obtained by another procedure in the next section. In that section a loop of any radius but of constant current will be analyzed. Closed form solutions will be possible only in the far-field region. The small loop far-field expressions will then be obtained as a special case of that problem.

Example 5.3

The radius of a small loop of constant current is $\lambda/25$. Find the physical area of the loop and compare it with its maximum effective aperture.

SOLUTION

$$S \text{ (physical)} = \pi a^2 = \pi\left(\frac{\lambda}{25}\right)^2 = \frac{\pi\lambda^2}{625} = 5.03 \times 10^{-3}\lambda^2$$

$$A_{em} = \frac{3\lambda^2}{8\pi} = 0.119\lambda^2$$

$$\frac{A_{em}}{S} = \frac{0.119\lambda^2}{5.03 \times 10^{-3}\lambda^2} = 23.66$$

Electrically the loop is about 24 times larger than its physical size, which should not be surprising. To be effective, a small loop must be larger electrically than its physical size.

5.2.7 Equivalent Circuit

A small loop is primarily inductive, and it can be represented by a lumped element equivalent circuit similar to those of Figure 2.22.

A. Transmitting Mode

The equivalent circuit for its input impedance when the loop is used as a transmitting antenna is that shown in Figure 5.3. This is similar to the equivalent circuit of Figure 2.22(b). Therefore its input impedance Z_{in} is represented by

$$Z_{\text{in}} = R_{\text{in}} + jX_{\text{in}} = (R_r + R_L) + j(X_A + X_i) \tag{5-33}$$

where

R_r = radiation resistance as given by (5-24)
R_L = loss resistance of loop conductor
X_A = external inductive reactance of loop antenna = ωL_A
X_i = internal high-frequency reactance of loop conductor = ωL_i

In Figure 5.3 the capacitor C_r is used in parallel to (5-33) to resonate the antenna; it can also be used to represent distributed stray capacitances. In order to determine the capacitance of C_r at resonance, it is easier to represent (5-33) by its equivalent admittance Y_{in} of

$$Y_{\text{in}} = G_{\text{in}} + jB_{\text{in}} = \frac{1}{Z_{\text{in}}} = \frac{1}{R_{\text{in}} + jX_{\text{in}}} \tag{5-34}$$

where

$$G_{\text{in}} = \frac{R_{\text{in}}}{R_{\text{in}}^2 + X_{\text{in}}^2} \tag{5-34a}$$

$$B_{\text{in}} = -\frac{X_{\text{in}}}{R_{\text{in}}^2 + X_{\text{in}}^2} \tag{5-34b}$$

At resonance, the susceptance B_r of the capacitor C_r must be chosen to eliminate the imaginary part B_{in} of (5-34) and (5-34a). This is accomplished by choosing C_r according to

$$C_r = \frac{B_r}{2\pi f} = -\frac{B_{\text{in}}}{2\pi f} = \frac{1}{2\pi f}\frac{X_{\text{in}}}{R_{\text{in}}^2 + X_{\text{in}}^2} \tag{5-35}$$

Under resonance the input impedance Z'_{in} is then equal to

$$Z'_{\text{in}} = R'_{\text{in}} = \frac{1}{G_{\text{in}}} = \frac{R_{\text{in}}^2 + X_{\text{in}}^2}{R_{\text{in}}} = R_{\text{in}} + \frac{X_{\text{in}}^2}{R_{\text{in}}} \tag{5-36}$$

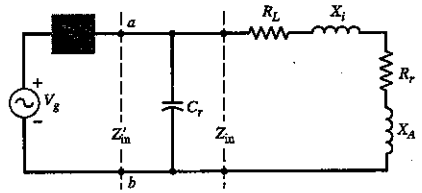

Figure 5.3 Equivalent circuit of loop antenna in transmitting mode.

The loss resistance R_L of the loop conductor can be computed using techniques illustrated in Example 5.2. The inductive reactance X_A of the loop is computed using the inductance L_A of:

Circular loop of radius a and wire radius b:

$$L_A = \mu_0 a\left[\ln\left(\frac{8a}{b}\right) - 2\right] \tag{5-37a}$$

Square loop with sides a and wire radius b:

$$L_A = 2\mu_0\frac{a}{\pi}\left[\ln\left(\frac{a}{b}\right) - 0.774\right] \tag{5-37b}$$

The internal reactance of the loop conductor X_i can be found using the internal inductance L_i of the loop which for a single turn can be approximated by

$$L_i = \frac{l}{\omega P}\sqrt{\frac{\omega\mu_0}{2\sigma}} = \frac{a}{\omega b}\sqrt{\frac{\omega\mu_0}{2\sigma}} \tag{5-38}$$

where l is the length and P is the perimeter of the wire of the loop

B. Receiving Mode

The loop antenna is often used as a receiving antenna or as a probe to measure magnetic flux density. Therefore when a plane wave impinges upon it, as shown in Figure 5.4(a), an open-circuit voltage develops across its terminals. This open-circuit voltage is related according to (2-93) to its vector effective length and incident electric field. This open-circuit voltage is proportional to the incident magnetic flux density B_z^i, which is normal to the plane of the loop. Assuming the incident field is uniform over the plane of the loop, the open-circuit voltage for a single-turn loop can be written as [5]

$$V_{oc} = j\omega\pi a^2 B_z^i \tag{5-39}$$

Defining in Figure 5.4(a) the plane of incidence as the plane formed by the z axis and radical vector, then the open-circuit voltage of (5-39) can be related to the magnitude of the incident magnetic and electric fields by

$$V_{oc} = j\omega\pi a^2\mu_0 H^i \cos\psi_i \sin\theta_i = jk_0\pi a^2 E^i \cos\psi_i \sin\theta_i \tag{5-39a}$$

where ψ_i is the angle between the direction of the magnetic field of the incident plane wave and the plane of incidence, as shown in Figure 5.4(a).

Since the open-circuit voltage is also related to the vector effective length by (2-93), then the effective length for a single turn loop can be written as

$$\ell_e = \hat{\mathbf{a}}_\phi l_e = \hat{\mathbf{a}}_\phi jk_0\pi a^2 \cos\psi_i \sin\theta_i = \hat{\mathbf{a}}_\phi jk_0 S \cos\psi_i \sin\theta_i \tag{5-40}$$

where S is the area of the loop. The factor $\cos\psi_i \sin\theta_i$ is introduced because the open-circuit voltage is proportional to the magnetic flux density component B_z^i which is normal to the plane of the loop.

When a load impedance Z_L is connected to the output terminals of the loop as shown in Figure 5.4(b), the voltage V_L across the load impedance Z_L is related to the input impedance Z_{in}' of Figure 5.4(b) and the open-circuit voltage of (5-39a) by

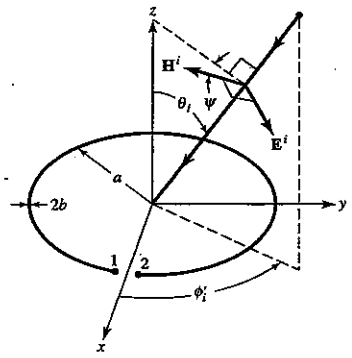

(a) Plane wave incident on a receiving loop (G.S. Smith, "Loop Antennas," Copyright © 1984, McGraw-Hill, Inc. Permission by McGraw-Hill, Inc.)

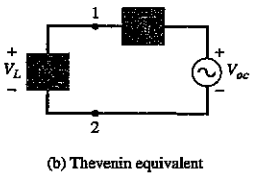

(b) Thevenin equivalent

Figure 5.4 Loop antenna and its equivalent in receiving mode.

$$V_L = V_{oc}\frac{Z_L}{Z_{in}' + Z_L} \tag{5-41}$$

5.3 CIRCULAR LOOP OF CONSTANT CURRENT

Let us now reconsider the loop antenna of Figure 5.1(a) but with a radius that may not necessarily be small. The current in the loop will again be assumed to be constant, as given by (5-1). For this current distribution, the vector potential is given by (5-14). Without using the small radius approximation, the integration in (5-14) cannot be carried out. However, if the observations are restricted in the far-field ($r \gg a$) region, the small radius approximation is not needed to integrate (5-14).

Although the uniform current distribution along the perimeter of the loop is only valid provided the circumference is less than about 0.2λ (radius less than about 0.03λ), the procedure developed here for a constant current can be followed to find the far zone fields of any size loop with not necessarily uniform current.

5.3.1 Radiated Fields

To find the fields in the far-field region, the distance R can be approximated by

$$R = \sqrt{r^2 + a^2 - 2ar\sin\theta\cos\phi'} \simeq \sqrt{r^2 - 2ar\sin\theta\cos\phi'} \quad \text{for} \quad r \gg a \tag{5-42}$$

which can be reduced, using the binomial expansion, to

$$\left.\begin{aligned} R &\simeq r\sqrt{1 - \frac{2a}{r}\sin\theta\cos\phi'} = r - a\sin\theta\cos\phi' = r - a\cos\psi_0 \\ &\qquad\qquad\qquad\qquad\qquad\qquad \text{for phase terms} \\ R &\simeq r \qquad\qquad\qquad\qquad\qquad\qquad \text{for amplitude terms} \end{aligned}\right\} \tag{5-43}$$

since

$$\cos\psi_0 = \hat{\mathbf{a}}_\rho' \cdot \hat{\mathbf{a}}_r \big|_{\phi=0} = (\hat{\mathbf{a}}_x \cos\phi' + \hat{\mathbf{a}}_y \sin\phi') \cdot (\hat{\mathbf{a}}_x \sin\theta\cos\phi + \hat{\mathbf{a}}_y \sin\theta\sin\phi + \hat{\mathbf{a}}_z \cos\theta)\big|_{\phi=0} = \sin\theta\cos\phi' \tag{5-43a}$$

The geometrical relation between R and r, for any observation angle ϕ in the far-field region, is shown in Figure 5.1(b). For observations at $\phi = 0$, it simplifies to that given by (5-43) and shown in Figure 5.5. Thus (5-14) can be written as

$$A_\phi \simeq \frac{a\mu I_0 e^{-jkr}}{4\pi r}\int_0^{2\pi} \cos\phi' e^{+jka\sin\theta\cos\phi'}\, d\phi' \tag{5-44}$$

and it can be separated into two terms as

$$A_\phi \simeq \frac{a\mu I_0 e^{-jkr}}{4\pi r}\left[\int_0^{\pi} \cos\phi' e^{+jka\sin\theta\cos\phi'}\, d\phi' + \int_{\pi}^{2\pi} \cos\phi' e^{+jka\sin\theta\cos\phi'}\, d\phi'\right] \tag{5-45}$$

The second term within the brackets can be rewritten by making a change of variable of the form

$$\phi' = \phi'' + \pi \tag{5-46}$$

Thus (5-45) can also be written as

$$A_\phi \simeq \frac{a\mu I_0 e^{-jkr}}{4\pi r}\left[\int_0^{\pi} \cos\phi' e^{+jka\sin\theta\cos\phi'}\, d\phi' - \int_0^{\pi} \cos\phi'' e^{-jka\sin\theta\cos\phi''}\, d\phi''\right] \tag{5-47}$$

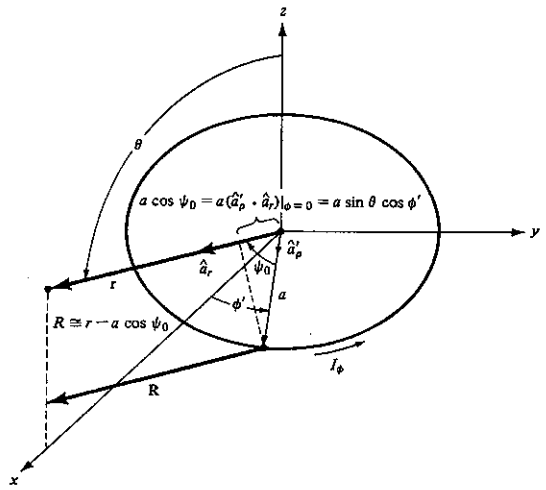

Figure 5.5 Geometry for far-field analysis of a loop antenna.

Each of the integrals in (5-47) can be integrated by the formula (see Appendix V)

$$\pi j^n J_n(z) = \int_0^{\pi} \cos(n\phi) e^{+jz\cos\phi}\, d\phi \tag{5-48}$$

where $J_n(z)$ is the Bessel function of the first kind of order n. Using (5-48) reduces (5-47) to

$$A_\phi \simeq \frac{a\mu I_0 e^{-jkr}}{4\pi r}[\pi j J_1(ka\sin\theta) - \pi j J_1(-ka\sin\theta)] \tag{5-49}$$

The Bessel function of the first kind and order n is defined (see Appendix V) by the infinite series

$$J_n(z) = \sum_{m=0}^{\infty} \frac{(-1)^m (z/2)^{n+2m}}{m!(m+n)!} \tag{5-50}$$

By a simple substitution into (5-50), it can be shown that

$$J_n(-z) = (-1)^n J_n(z) \tag{5-51}$$

which for $n = 1$ is equal to

$$J_1(-z) = -J_1(z) \tag{5-52}$$

Using (5-52) we can write (5-49) as

$$A_\phi \simeq j\frac{a\mu I_0 e^{-jkr}}{2r} J_1(ka\sin\theta) \tag{5-53}$$

The next step is to find the **E**- and **H**-fields associated with the vector potential of (5-53). Since (5-53) is only valid for far-field observations, the procedure outlined in Section 3.6 can be used. The vector potential **A**, as given by (5-53), is of the form suggested by (3-56). That is, the r variations are separable from those of θ and ϕ. Therefore according to (3-58a)–(3-58b) and (5-53)

$$E_r \simeq E_\theta = 0 \tag{5-54a}$$

$$E_\phi \simeq \frac{ak\eta I_0 e^{-jkr}}{2r} J_1(ka\sin\theta) \tag{5-54b}$$

$$H_r \simeq H_\phi = 0 \tag{5-54c}$$

$$H_\theta \simeq -\frac{E_\phi}{\eta} = -\frac{akI_0 e^{-jkr}}{2r} J_1(ka\sin\theta) \tag{5-54d}$$

5.3.2 Power Density, Radiation Intensity, Radiation Resistance, and Directivity

The next objective for this problem will be to find the power density, radiation intensity, radiation resistance, and directivity. To do this, the time-average power density is formed. That is,

$$\mathbf{W}_{av} = \frac{1}{2}\text{Re}[\mathbf{E}\times\mathbf{H}^*] = \frac{1}{2}\text{Re}\,[\hat{\mathbf{a}}_\phi E_\phi \times \hat{\mathbf{a}}_\theta H_\theta^*] = \hat{\mathbf{a}}_r \frac{1}{2\eta}|E_\phi|^2 \tag{5-55}$$

which can be written using (5-54b) as

$$\mathbf{W}_{av} = \hat{\mathbf{a}}_r W_r = \hat{\mathbf{a}}_r \frac{(a\omega\mu)^2|I_0|^2}{8\eta r^2} J_1^2(ka \sin\theta) \tag{5-56}$$

with the radiation intensity given by

$$U = r^2 W_r = \frac{(a\omega\mu)^2|I_0|^2}{8\eta} J_1^2(ka \sin\theta) \tag{5-57}$$

The radiation patterns for $a = \lambda/10$, $\lambda/5$, and $\lambda/2$ are shown in Figure 5.6. These patterns indicate that the field radiated by the loop along its axis ($\theta = 0°$) is zero. Also the shape of these patterns is similar to that of a linear dipole with $l \leq \lambda$ (a figure-eight shape). As the radius a increases beyond 0.5λ, the field intensity along the plane of the loop ($\theta = 90°$) diminishes and eventually it forms a null when $a \simeq 0.61\lambda$. This is left as an exercise to the reader for verification (Prob. 5.13). Beyond $a = 0.61\lambda$, the radiation along the plane of the loop begins to intensify and the pattern attains a multilobe form.

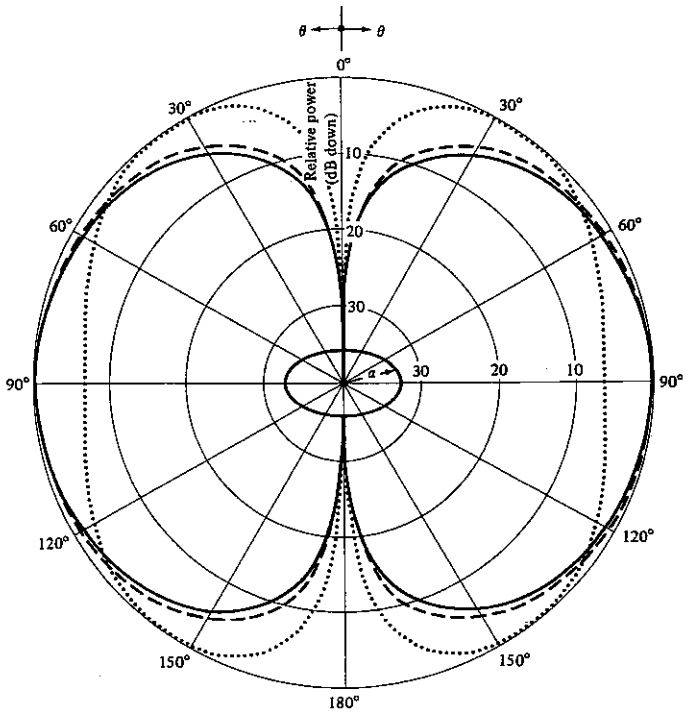

Figure 5.6 Elevation plane amplitude patterns for a circular loop of constant current ($a = 0.1\lambda$, 0.2λ, and 0.5λ).

The patterns represented by (5-57) (some of them are illustrated in Figure 5.6) assume that the current distribution, no matter what the loop size, is constant. This is not a valid assumption if the loop circumference C ($C = 2\pi a$) exceeds about 0.2λ (i.e., $a > 0.032\lambda$) [6]. For radii much greater than about 0.032λ, the current variation along the circumference of the loop begins to attain a distribution that is best represented by a Fourier series [5]. Although a most common assumption is that the current distribution is nearly cosinusoidal, it is not satisfactory particulary near the driving point of the antenna.

It has been shown [7] that when the circumference of the loop is about one wavelength ($C = \lambda$), its maximum radiation is along its axis ($\theta = 0°$) which is perpendicular to the plane of the loop. This feature of the loop antenna has been utilized to design Yagi-Uda arrays whose basic elements (feed, directors, and reflectors) are circular loops [8]–[10]. Because of its many applications, the one wavelength circumference circular loop antenna is considered as fundamental as a half-wavelength dipole.

The radiated power can be written using (5-56) as

$$P_{rad} = \iint_S \mathbf{W}_{av} \cdot d\mathbf{s} = \frac{\pi(a\omega\mu)^2|I_0|^2}{4\eta} \int_0^{\pi} J_1^2(ka \sin\theta) \sin\theta \, d\theta \tag{5-58}$$

The integral in (5-58) cannot be integrated exactly. However, it can be rewritten [11] as

$$\int_0^{\pi} J_1^2(ka \sin\theta) \sin\theta \, d\theta = \frac{1}{ka} \int_0^{2ka} J_2(x) \, dx \tag{5-59}$$

Even though (5-59) still cannot be integrated, approximations can be made depending upon the values of the upper limit (the radius of the loop).

A. Large Loop Approximation ($a \geq \lambda/2$)

To evaluate (5-59), the first approximation will be to assume that the radius of the loop is large ($a \geq \lambda/2$). For that case, the integral in (5-59) can be approximated by

$$\int_0^{\pi} J_1^2(ka \sin\theta) \sin\theta \, d\theta = \frac{1}{ka} \int_0^{2ka} J_2(x) \, dx \simeq \frac{1}{ka} \tag{5-60}$$

and (5-58) by

$$P_{rad} \simeq \frac{\pi(a\omega\mu)^2|I_0|^2}{4\eta(ka)} \tag{5-61}$$

The maximum radiation intensity occurs when $ka \sin\theta = 1.84$ so that

$$U|_{max} = \frac{(a\omega\mu)^2|I_0|^2}{8\eta} J_1^2(ka \sin\theta)|_{ka\sin\theta=1.84} = \frac{(a\omega\mu)^2|I_0|^2}{8\eta}(0.584)^2 \tag{5-62}$$

Thus

$$R_r = \frac{2P_{\text{rad}}}{|I_0|^2} = \frac{2\pi(a\omega\mu)^2}{4\eta(ka)} = \eta\left(\frac{\pi}{2}\right)ka = 60\pi^2(ka) = 60\pi^2\left(\frac{C}{\lambda}\right) \quad (5\text{-}63a)$$

$$D_0 = 4\pi\frac{U_{\max}}{P_{\text{rad}}} = 4\pi\frac{ka(0.584)^2}{2\pi} = 2ka(0.584)^2 = 0.682\left(\frac{C}{\lambda}\right) \quad (5\text{-}63b)$$

$$A_{em} = \frac{\lambda^2}{4\pi}D_0 = \frac{\lambda^2}{4\pi}\left[0.682\left(\frac{C}{\lambda}\right)\right] = 5.43 \times 10^{-2}\lambda C \quad (5\text{-}63c)$$

where C (circumference) $= 2\pi a$ and $\eta \simeq 120\pi$.

B. Intermediate Loop Approximation ($\lambda/6\pi \leq a < \lambda/2$)

If the radius of the loop is $\lambda/6\pi \leq a < \lambda/2$, the integral of (5-59) can be approximated by

$$\int_0^{\pi} J_1^2(ka\sin\theta)\sin\theta\, d\theta = \frac{1}{ka}\int_0^{2ka} J_2(x)\, dx \simeq \frac{1}{ka}\left[-2J_1(2ka) + \int_0^{2ka} J_0(y)\, dy\right] \quad (5\text{-}64)$$

where $J_0(y)$ is the Bessel function of the first kind of zero order. No further simplifications can be made. The integral of $J_0(y)$ appearing in (5-64) is a tabulated function which is included in Appendix V. The radiation resistance, directivity, and maximum effective area can be found using (5-64) to evaluate the P_{rad} of (5-58).

C. Small Loop Approximation ($a < \lambda/6\pi$)

If the radius of the loop is small ($a < \lambda/6\pi$), the expressions for the fields as given by (5-54a)–(5-54d) can be simplified. To do this, the Bessel function $J_1(ka\sin\theta)$ is expanded, by the definition of (5-50), in an infinite series of the form (see Appendix V)

$$J_1(ka\sin\theta) = \tfrac{1}{2}(ka\sin\theta) - \tfrac{1}{16}(ka\sin\theta)^3 + \cdots \quad (5\text{-}65)$$

For small values of ka ($ka < \frac{1}{3}$), (5-65) can be approximated by its first term, or

$$J_1(ka\sin\theta) \simeq \frac{ka\sin\theta}{2} \quad (5\text{-}65a)$$

Thus (5-54a)–(5-54d) can be written as

$$\left.\begin{aligned} E_r &\simeq E_\theta = 0 && (5\text{-}66a)\\ E_\phi &\simeq \frac{a^2\omega\mu k I_0 e^{-jkr}}{4r}\sin\theta = \eta\frac{a^2k^2I_0e^{-jkr}}{4r}\sin\theta && (5\text{-}66b)\\ H_r &\simeq H_\phi = 0 && (5\text{-}66c)\\ H_\theta &\simeq -\frac{a^2\omega\mu k I_0 e^{-jkr}}{4\eta r}\sin\theta = -\frac{a^2k^2I_0e^{-jkr}}{4r}\sin\theta && (5\text{-}66d)\end{aligned}\right\} a < \lambda/6\pi$$

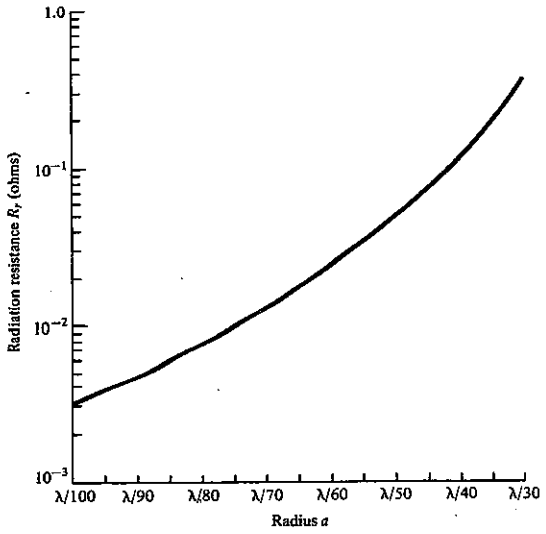

Figure 5.7 Radiation resistance for a constant current circular loop antenna based on the approximation of (5-65a).

which are identical to those of (5-27a)–(5-27c). Thus the expressions for the radiation resistance, radiation intensity, directivity, maximum effective aperture, and radiation resistance are those given by (5-24), (5-29), (5-31), and (5-32).

To demonstrate the variation of the radiation resistance as a function of the radius a of the loop, it is plotted in Figure 5.7 for $\lambda/100 \leq a \leq \lambda/30$, based on the approximation of (5-65a). It is evident that the values are extremely low (less than 1 ohm), and they are usually smaller than the loss resistances of the wires. These radiation resistances also lead to large mismatch losses when connected to practical transmission lines of 50 or 75 ohms. To increase the radiation resistance, it would require multiple turns as suggested by (5-24a). This, however, also increases the loss resistance which contributes to the inefficiency of the antenna. A plot of the radiation resistance for $0 < ka = C/\lambda < 20$, based on the evaluation of (5-59) by numerical techniques, is shown in Figure 5.8. The dashed line represents the values based on the large loop approximation of (5-60) and the dotted (· · · · ·) represents the values based on the small loop approximation of (5-65a).

In addition to the real part of the input impedance, there is also an imaginary component which would increase the mismatch losses even if the real part is equal to the characteristic impedance of the lossless transmission line. However, the imaginary component can always, in principle at least, be eliminated by connecting a reactive element (capacitive or inductive) across the terminals of the loop to make the antenna a resonant circuit.

To facilitate the computations for the directivity and radiation resistance of a circular loop with a constant current distribution, a FORTRAN computer program has

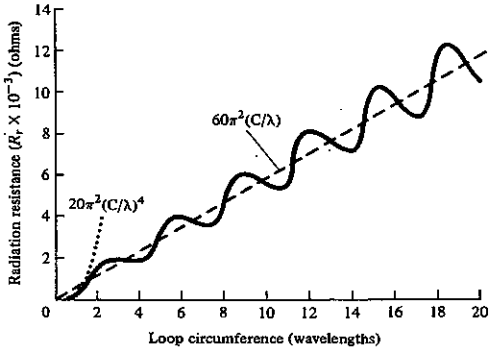

(a) Radiation resistance of circular loop

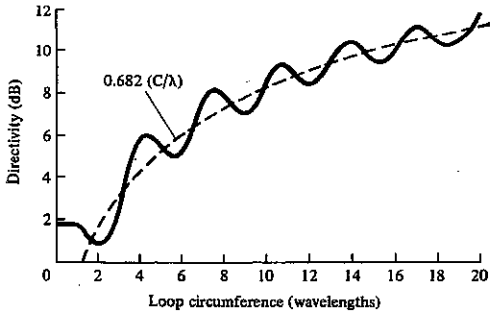

(b) Directivity of circular loop

Figure 5.8 Radiation resistance and directivity for circular loop of constant current. (SOURCE: E. A. Wolff, *Antenna Analysis*, Wiley, New York, 1966)

been developed. The program utilizes (5-62) and (5-58) to compute the directivity [(5-58) is integrated numerically]. The program requires as an input the radius of the loop (in wavelengths). A Bessel function subroutine is contained within the program. A listing of the program is included at the end of this chapter and in the computer disc included with the book.

5.4 CIRCULAR LOOP WITH NONUNIFORM CURRENT

The analysis in the previous sections was based on a uniform current, which would be a valid approximation when the radius of the loop is small electrically (usually $a < 0.03\lambda$). As the dimensions of the loop increase, the current variations along the circumference of the loop must be taken into account. As stated previously, a very common assumption for the current distribution is a cosinusoidal variation [12], [13]. This, however, is not a satisfactory approximation particularly near the driving point

of the antenna [6]. A better distribution would be to represent the current by a Fourier series [14]

$$I(\phi') = I_0 + 2\sum_{n=1}^{M} I_n \cos(n\phi') \tag{5-67}$$

where ϕ' is measured from the feed point of the loop along the circumference, as shown at the inset of Figure 5.9.

A complete analysis of the fields radiated by a loop with nonuniform current distribution is somewhat complex, laborious, and quite lengthy. Instead of attempting to include the analytical formulations, which are cumbersome but well documented in the cited references, a number of graphical illustrations of numerical and experimental data is presented. These curves can be used in facilitating designs.

To illustrate that the current distribution of a wire loop antenna is not uniform unless its radius is very small, the magnitude and phase of it have been plotted in Figure 5.9 as a function of ϕ' (in degrees). The loop circumference C is $ka = C/\lambda$

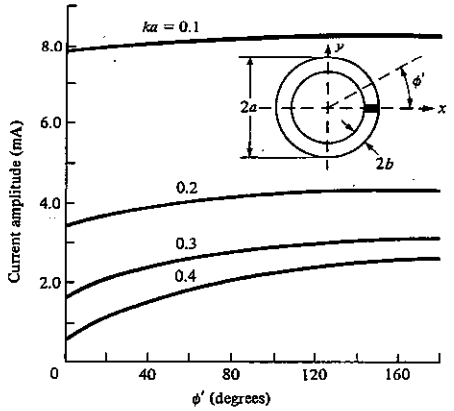

(a) Magnitude

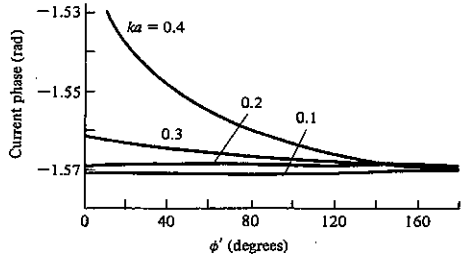

(b) Phase

Figure 5.9 Current magnitude and phase distributions on small circular loop antennas. (SOURCE: J. E. Storer, "Impedance of Thin-Wire Loop Antennas," *AIEE Trans.*, Vol. 75, November 1956. © 1956 IEEE)

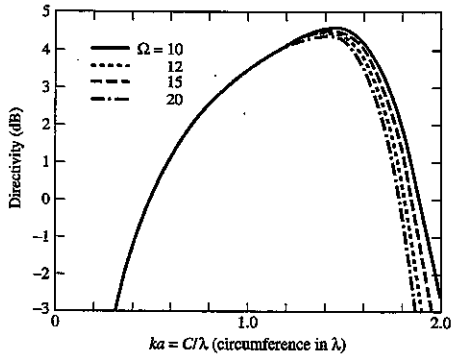

Figure 5.10 Directivity of circular-loop antenna for $\theta = 0, \pi$ versus electrical size (circumference/wavelength). (SOURCE: G. S. Smith, "Loop Antennas," copyright © McGraw-Hill, Inc. Permission by McGraw-Hill, Inc.)

$= 0.1$, 0.2, 0.3, and 0.4 and the wire size was chosen so that $\Omega = 2\ln(2\pi a/b) = 10$. It is apparent that for $ka = 0.1$ the current is nearly uniform. For $ka = 0.2$ the variations are slightly greater and become even larger as ka increases. On the basis of these results, loops much larger than $ka = 0.2$ (radius much greater than 0.03–0.04λ) cannot be considered small.

As was indicated earlier, the maximum of the pattern for a loop antenna shifts from the plane of the loop ($\theta = 90°$) to its axis ($\theta = 0°, 180°$) as the circumference of the loop approaches one wavelength. Based on the nonuniform current distribution of (5-67), the directivity of the loop along $\theta = 0°$ has been computed, and it is plotted in Figure 5.10 versus the circumference of the loop in wavelengths [5]. The maximum directivity is about 4.5 dB, and it occurs when the circumference is about 1.4λ. For a one wavelength circumference, which is usually the optimum design for a helical antenna, the directivity is about 3.4 dB. It is also apparent that the directivity is basically independent of the radius of the wire, as long as the circumference is equal or less than about 1.3 wavelengths; there are differences in directivity as a function of the wire radius for greater circumferences.

Computed impedances, based on the Fourier series representation of the current, are shown plotted in Figure 5.11. The input resistance and reactance are plotted as a function of the circumference C (in wavelengths) for $0 \le ka = C/\lambda \le 2.5$. The diameter of the wire was chosen so that $\Omega = 2\ln(2\pi a/b) = 8, 9, 10, 11$, and 12. It is apparent that the first antiresonance occurs when the circumference of the loop is about $\lambda/2$, and it is extremely sharp. It is also noted that as the loop wire increases in thickness, there is a rapid disappearance of the resonances. As a matter of fact, for $\Omega < 9$ there is only one antiresonance point. These curves (for $C > \lambda$) are similar, both qualitatively and quantitatively, to those of a linear dipole. The major difference is that the loop is more capacitive (by about 130 ohms) than a dipole. This shift in reactance allows the dipole to have several resonances and antiresonances while moderately thick loops ($\Omega < 9$) have only one antiresonance. Also small loops are primarily inductive while small dipoles are primarily capacitive. The resistance curves for the loop and the dipole are very similar.

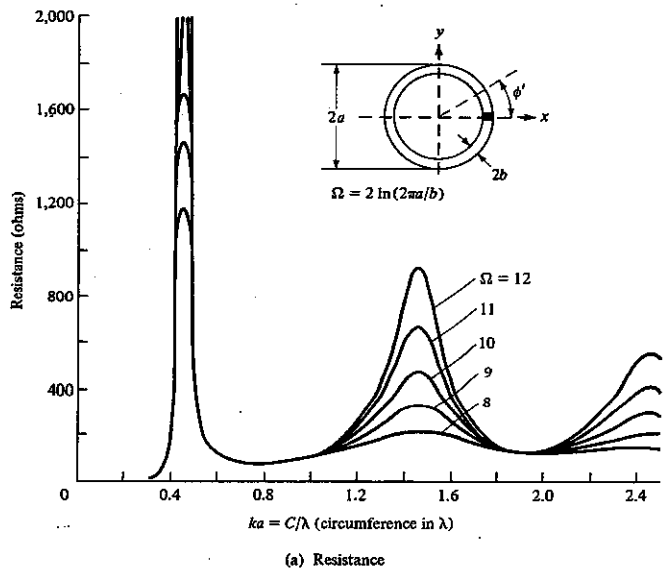

(a) Resistance

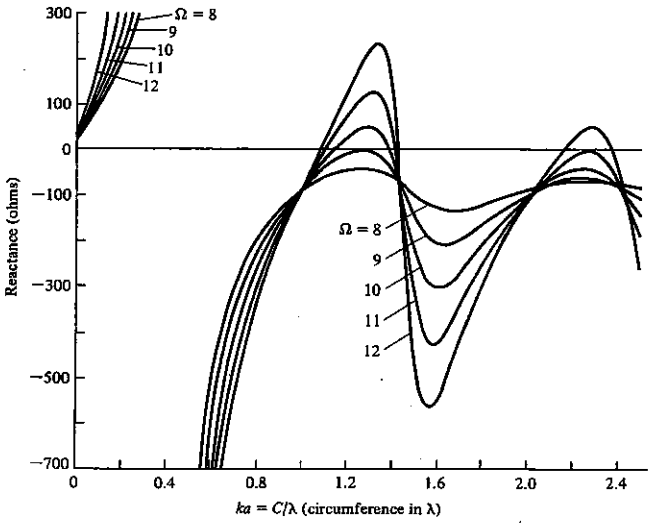

(b) Reactance

Figure 5.11 Input impedance of circular loop antennas. (SOURCE: J. E. Stover, "Impedance of Thin-Wire Loop Antennas," *AIEE Trans.*, Vol. 75, November 1956. © 1956 IEEE).

To verify the analytical formulations and the numerical computations, loop antennas were built and measurements of impedance were made [6]. The measurements were conducted using a half-loop over an image plane, and it was driven by a two-wire line. An excellent agreement between theory and experiment was indicated everywhere except near resonances where computed conductance curves were slightly higher than those measured. This is expected since ohmic losses were not taken into account in the analytical formulation. It was also noted that the measured susceptance curve was slightly displaced vertically by a constant value. This can be attributed to the "end effect" of the experimental feeding line and the "slice generator" used in the analytical modeling of the feed. For a dipole, the correction to the analytical model is usually a negative capacitance in shunt with the antenna [15]. A similar correction for the loop would result in a better agreement between the computed and measured susceptances. Computations for a half-loop above a ground plane were also performed by J. E. Jones [16] using the Moment Method.

The radiation resistance of a loop antenna, with a cosinusoidal current distribution, was computed [17] by evaluating triple integrals numerically. The results are shown in Figure 5.12 where they are compared with those of a uniform current distribution. It is evident that when the circumference of the loop is less than about 0.8λ, the constant current radiation resistances agree quite well with those of the cosinusoidal distribution.

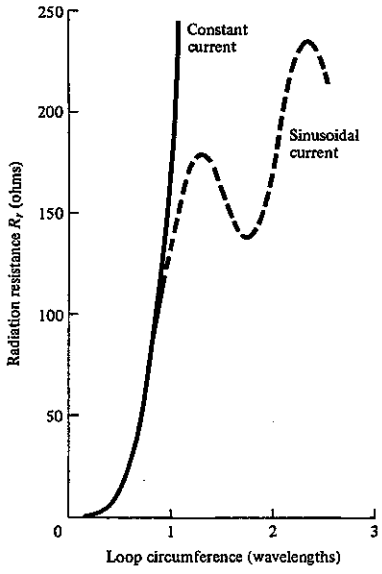

Figure 5.12 Radiation resistance of circular loop with constant and sinusoidal current distributions. (SOURCE: A. Richtscheid, "Calculation of the Radiation Resistance of Loop Antennas with Sinusoidal Current Distribution," *IEEE Trans. Antennas Propagat.*, Vol. AP-24, November 1976. © 1976 IEEE)

5.4.1 Arrays

In addition to be used as single elements, loop antennas are widely used in arrays. Two of the most popular arrays of loop antennas are the helical antenna and the Yagi-Uda array. The loop is also widely used to form a solenoid which in conjunction with a ferrite cylindrical rod within its circumference is used as a receiving antenna and as a tuning element, especially in transistor radios. This is discussed in Section 5.7.

The helical antenna, which is discussed in more detail in Section 10.3.1, is a wire antenna, which is wound in the form of a helix, as shown in Figure 10.13. It is shown that it can be modeled approximately by a series of loops and vertical dipoles, as shown in Figure 10.14. The helical antenna possesses in general elliptical polarization, but it can be designed to achieve nearly circular polarization. There are two primary modes of operation for a helix, the normal mode and the axial mode. The helix operates in its normal mode when its overall length is small compared to the wavelength, and it has a pattern with a null along its axis and the maximum along the plane of the loop. This pattern (figure eight type in the elevation plane) is similar to that of a dipole or a small loop. The helix operates in the axial mode when the circumference of the loop is between $3/4\lambda < C < 4/3\lambda$ with an optimum design when the circumference is nearly one wavelength. When the circumference of the loop approaches one wavelength, the maximum of the pattern is along its axis. In addition, the phasing among the turns is such that overall the helix forms an end-fire antenna with attractive impedance and polarization characteristics. In general, the helix is a popular communication antenna in the VHF and UHF bands.

The Yagi-Uda antenna is primarily an array of linear dipoles with one element serving as the feed while the others act as parasitic. However this arrangement has been extended to include arrays of loop antennas, as shown in Figure 10.27. As for the helical antenna, in order for this array to perform as an endfire array, the circumference of each of the elements is near one wavelength. More details can be found in Section 10.3.4 and especially in [8]–[10]. A special case is the quad antenna which is very popular amongst ham radio operators. It consists of two square loops, one serving as the excitation while the other is acting as a reflector; there are no directors. The overall perimeter of each loop is one wavelength.

5.4.2 Design Procedure

The design of small loops is based on the equations for the radiation resistance (5-24), (5-24a), directivity (5-31), maximum effective aperture (5-32), resonance capacitance (5-35), resonance input impedance (5-36) and inductance (5-37a), (5-37b). In order to resonate the element, the capacitor C_r of Figure 5.3 is chosen based on (5-35) so as to cancel out the imaginary part of the input impedance Z_{in}.

For large loops with a nonuniform current distribution, the design is accomplished using the curves of Figure 5.10 for the axial directivity and those of Figure 5.11 for the impedance. To resonate the loop, usually a capacitor in parallel or an inductor in series is added, depending on the radius of the loop and that of the wire.

Example 5.4

Design a resonant loop antenna to operate at 100 MHz so that the pattern maximum is along the axis of the loop. Determine the radius of the loop and that of the wire (in